



Contents lists available at ScienceDirect

# Journal of Quantitative Spectroscopy & Radiative Transfer

journal homepage: [www.elsevier.com/locate/jqsrt](http://www.elsevier.com/locate/jqsrt)

## Fluorescence spectra and biological activity of aerosolized *Bacillus* spores and MS2 bacteriophage exposed to ozone at different relative humidities in a rotating drum



Shanna Ratnesar-Shumate<sup>a,b</sup>, Yong-Le Pan<sup>c</sup>, Steven C. Hill<sup>c</sup>, Sean Kinahan<sup>a</sup>, Elizabeth Corson<sup>a</sup>, Jonathan Eshbaugh<sup>a</sup>, Joshua L. Santarpia<sup>b,d,\*</sup>

<sup>a</sup> The Johns Hopkins University Applied Physics Laboratory, 11100 Johns Hopkins Road, Laurel, MD, USA

<sup>b</sup> The University of Maryland Baltimore County, 1000 Hilltop Cir, Baltimore, MD 21250, USA

<sup>c</sup> US Army Research Laboratory, 2800 Powder Mill Road, Adelphi, MD 20783, USA

<sup>d</sup> Sandia National Laboratory, 1515 Eubank SE, Albuquerque, NM 87123, USA

### ARTICLE INFO

#### Article history:

Received 6 May 2014

Received in revised form

29 September 2014

Accepted 4 October 2014

Available online 14 October 2014

#### Keywords:

Bioaerosols

Spectroscopy

*Bacillus*

Bacteriophage

Ozone

Relative humidity

### ABSTRACT

Biological aerosols (bioaerosols) released into the environment may undergo physical and chemical transformations when exposed to atmospheric constituents such as solar irradiation, reactive oxygenated species, ozone, free radicals, water vapor and pollutants. Aging experiments were performed in a rotating drum chamber subjecting bioaerosols, *Bacillus thuringiensis* Al Hakam (BtAH) spores and MS2 bacteriophages to ozone at 0 and 150 ppb, and relative humidities (RH) at 10%, 50%, and 80+%. Fluorescence spectra and intensities of the aerosols as a function of time in the reaction chamber were measured with a single particle fluorescence spectrometer (SPFS) and an Ultra-Violet Aerodynamic Particle Sizer<sup>®</sup> Spectrometer (UV-APS). Losses in biological activity were measured by culture and quantitative polymerase chain reaction (q-PCR) assay. For both types of aerosols the largest change in fluorescence emission was between 280 and 400 nm when excited at 263 nm followed by fluorescence emission between 380 and 700 nm when excited at 351 nm. The fluorescence for both BtAH and MS2 were observed to decrease significantly at high ozone concentration and high RH when excited at 263 nm excitation. The decreases in 263 nm excited fluorescence are indicative of hydrolysis and oxidation of tryptophan in the aerosols. Fluorescence measured with the UV-APS (355-nm excitation) increased with time for both BtAH and MS2 aerosols. A two log loss of MS2 bacteriophage infectivity was observed in the presence of ozone at ~50% and 80% RH when measured by culture and normalized for physical losses by q-PCR. Viability of BtAH spores after exposure could not be measured due to the loss of genomic material during experiments, suggesting degradation of extracellular DNA attributable to oxidation. The results of these studies indicate that the physical and biological properties of bioaerosols change significantly after exposure to ozone and water vapor.

© 2014 The Authors. Published by Elsevier Ltd. This is an open access article under the CC BY-NC-ND license (<http://creativecommons.org/licenses/by-nc-nd/3.0/>).

\* Corresponding author at: Sandia National Laboratory, 1515 Eubank SE, Albuquerque, NM 87123, USA.

E-mail address: [jsantar@sandia.gov](mailto:jsantar@sandia.gov) (J.L. Santarpia).

<http://dx.doi.org/10.1016/j.jqsrt.2014.10.003>

0022-4073/© 2014 The Authors. Published by Elsevier Ltd. This is an open access article under the CC BY-NC-ND license (<http://creativecommons.org/licenses/by-nc-nd/3.0/>).

### 1. Introduction

The atmosphere contains naturally occurring aerosols that fluctuate in concentration and composition. Biological

aerosols (bioaerosols) consist of airborne particles that may be alive or dead, may contain multiple organisms, or be released from living organisms [1]. Some examples of bioaerosols include bacteria, fungi, pollens, viruses, toxins, cell debris and plant matter [1,6,15,26]. The negative health effects of bioaerosols may be due to infectious pathogens, toxins produced by organisms, and/or may result from immunological reactions such as asthma [15]. Bioaerosols can serve as ice nuclei (IN) and cloud condensation nuclei (CCN). Due to their roles as IN and CCN bioaerosols may influence cloud coverage, precipitation patterns and rates, thereby affecting the global radiative balance [1,6]. Living bioaerosols have been shown to metabolize atmospheric organic compounds and oxidants, resulting in the production of new atmospheric chemical species [6,30].

Vegetative bacterial bioaerosols (e.g., *Escherichia coli*, *Serratia marcescens*, *Francisella tularensis*, *Brucella suis*, and *Staphylococcus epidermidis*) [19] and viruses [2] have been shown to be sensitive to components, known as “open air factors” (OAFs), in outdoor environments [5]. Other types of bacteria have been shown to be insensitive to OAFs including *Bacillus subtilis* and *Bacillus anthracis* spores and *Micrococcus radiodurans* [5,19]. OAF is hypothesized to be the result of exposure to ozone, olefins, and ozone–olefin reaction products [19]. De Mik and DeGroot [20] showed inactivation of the  $\phi$ X174 bacteriophage due to damaged proteins when exposed to either ozone or to cyclohexane. In combination, ozone and cyclohexane resulted in inactivation via damage to both proteins and DNA.

There are many other mechanisms by which bioaerosol particles may undergo chemical or physical changes in the atmosphere [6] including chemical reactions with nitrogen oxides, OH radicals, uptake of water or desiccation due to fluctuations in relative humidity (RH), solar irradiation initiated photochemical reactions, agglomeration with other aerosols and interactions with secondary aerosol forming precursors. In addition bioaerosols may also cause changes to other aerosols or chemicals in the atmosphere through metabolic interactions with organic compounds [1,6,30]. The effect of these mechanisms on and the roles of bioaerosols in the atmosphere is an ongoing topic of study.

Several kinds of sensors have been developed to detect and characterize bioaerosols. Identification of microbes to the genus or species level is accomplished using antibodies to specific proteins on cell or viral surfaces or via DNA/RNA identification using sequencing or polymerase chain reaction (PCR). Rapid reagentless detection methods based on intrinsic fluorescence of certain fluorophores have been developed and are commercially available [8,12,27,32,35]. Cells and most proteins contain tryptophan, which when excited by UV light emits fluorescence peaking between 310 and 350 nm. Additionally, cells contain NADH, which emits light in the 400–500 nm range [13,14] when excited by near-UV light. Chemical changes to bioaerosols caused by interactions with constituents in the atmosphere may diminish detectability in cases where specific molecules (e.g., tryptophan, nicotinamides, flavins, surface antigens, DNA) that are used for identification are modified [23,26]. The spectroscopic signature detected by a sensor is dependent on the wavelength used for generating the fluorescence (excitation

wavelength), the emitted fluorescence (spectrally resolved or in one or more bands occurring over some wavelength range) as well as the ratios of the fluorophores within the bioaerosol being interrogated. In many cases, light scattering from the particle is also used to infer size and shape information, which may aid in discrimination. Changes in detectability could result in misinterpretation of measurements and underestimation of bioaerosol concentrations in the environment.

Effects of ozone on the fluorescence properties of tryptophan in solution have been reported [16,17,21]. Santarpi et al. [26] showed significant fluorescence decreases in the 330 nm peak emission of *Yersinia rohdei* and MS2 bacteriophage aerosols, when excited at 263 nm in the presence of high concentrations of ozone (> 300 ppb) at relative humidity of 35–43%. Further, a more rapid decrease in the emission spectra was observed when relative humidity was increased by less than 7%, indicating that uptake of water by bioaerosols may be important in the facilitation of atmospheric changes to the spectral properties. Effects were seen before the product of time and concentration reached the 8-hour Environmental Protection Agency (EPA) limit for exposure to ozone. The observed changes in fluorescence in the 300 nm peak are in agreement with the effects of ozone on tryptophan fluorescence in solution as previously reported by Ignatenko et al. [16]. However, these experiments were performed at higher than typical ozone levels in the United States and with limited control over RH. Pan et al. [23] measured changes in spectra of eight-amino-acid-peptide aerosols containing one tryptophan, one tyrosine, and one phenylalanine per molecule, at atmospherically relevant ozone concentrations (0 or 150 ppb) at different RH levels (~20%, 50%, or 80%). The 263 nm fluorescence of the peptide in the 280–560 nm band was shown to decrease with time of exposure to ozone while the 351 nm excited fluorescence between 430 and 700 nm was shown to increase. Both these changes are consistent with the oxidation of tryptophan to *N*-formyl kynurenine (NF) and kynurenine (KY) [16,17,21]. These results indicate that there exists a potential for changes to the spectral properties of bioaerosols when exposed to atmospheric constituents, potentially impacting the ability of sensors to accurately detect them.

To understand the limitations of fluorescence-based measurements for detection and characterization of biological aerosols and to develop improved instrumentation and methods for making measurements, changes that may occur due to atmospheric exposure to ozone and water vapor need to be fully understood. This paper reports the spectral properties of ultra-violet laser-induced fluorescence (UV-LIF) of two types of biological aerosols, *Bacillus thuringiensis* Al Hakam (BtAH) spores and MS2 bacteriophage when excited at 263, 351, and 355 nm after exposure to ozone at different RH. In addition, measurement of the changes in biological activity of these bioaerosols as a function of the exposure conditions were attempted in order to correlate with loss in spectroscopic signatures.

## 2. Experimental methodology

Pan et al. [23] previously described the apparatus used for these experiments which utilized a rotating reaction

drum chamber, an aerosol generator, an ultraviolet aerodynamic particle sizer (UV-APS), a single particle fluorescence spectrometer (SPFS), and equipment to generate, monitor and control the ozone and RH. In summary, the rotating drum consisted of a 400L stainless steel cylindrical chamber rotating at 1 RPM with a chemically inert Teflon coated interior. The drum rotated around a center axle, containing sampling lines in which the aerosol and ozone were introduced and samples were drawn. More than 20% of the injected aerosols between 1 and 2  $\mu\text{m}$  in the drum remained suspended in the chamber for up to 4 hours. The concentration of ozone and the relative humidity were autonomously controlled to observe the corresponding changes in the aerosol. Water vapor was generated using a small piezo-electric water generator (Model # 50-1011.1, APC International Ltd.) housed in a custom made acrylic tube and placed directly inside the drum chamber. RH and temperature were monitored in the drum using a probe mounted along the center (Model # HMP110, Vaisala Inc.). Ozone was generated into the drum by passing laboratory air at 50 mL/min over a small mercury pen lamp (< 220 nm, Pen, Ray, 97-0067-01) housed within a Teflon enclosure. Air exiting the Teflon enclosure containing photolyzed oxygen converted into ozone was then delivered into the drum until the desired concentration was achieved. The concentration of ozone in the drum was measured using an ozone monitor (Model 106-L, 2B Technologies Inc.) sampling at 1 Lpm with a range of 0–100 ppm and a resolution of 0.1 ppb. The aerosol was generated and transported into the drum using an ultrasonic nozzle aerosol generation system consisting of a 120 kHz nozzle, broadband ultrasonic generator, and syringe pump (Models # 06-04010, #06-05108, 11-01061, Sono-Tek Corp.). The ultrasonic nozzle was housed in an Aerosol Capacitance Chamber (ACC) system [25].

A UV-APS (Model #3312, TSI Inc.) was used to measure the size distribution and fluorescence of biological aerosols during experiments. The UV-APS measured the integrated fluorescence (430–580 nm) of aerosols excited at 355 nm and reported the aerodynamic size of the aerosol between 0.523 and 20  $\mu\text{m}$ . Air was sampled into the UV-APS at 1 Lpm directly from the rotating drum with 4 Lpm of sheath air being drawn from the surrounding laboratory.

### 2.1. Single-particle fluorescence spectrometer

The single-particle fluorescence spectrometer (SPFS) was used to measure the LIF of individual bioaerosol particles from the rotating drum as a function of exposure to RH and ozone [23]. The aerosol was drawn into an 18 in.<sup>3</sup> airtight chamber at 1 L/min from the drum, and then focused into a laminar jet of around 300  $\mu\text{m}$  in diameter by a sheath nozzle within the chamber. Any aerosol particles larger than 1  $\mu\text{m}$  flowing through a trigger volume ( $\sim 100 \mu\text{m} \times 100 \mu\text{m}$  defined by the intersection of two diode-laser beams at 650 nm and 685 nm) were detected by two photomultiplier tubes (PMTs) and illuminated by a single pulse of 263-nm or 351-nm laser. Emitted fluorescence was collected by a reflective objective and dispersed by a spectrograph. Two long-pass filters with cut wavelengths at 280 nm and 365 nm installed in a filter wheel

mounted on the front of the spectrograph were used to block the elastic scattering of the laser at 263 and 351 nm, respectively. Both filters have about 95% transmission at 3 nm above the cut-off wavelength, and have a very steep cut-off at the indicated wavelength. An Image-Intensified Charge-Coupled (ICCD) camera recorded the dispersed spectrum. A third PMT and a diode laser at 705 nm were used for measuring the particle size. The near forward scattering ( $10\text{--}40^\circ$ ) was detected by the PMT, amplified, sent to a data acquisition board and digitized with the outputs recorded by the computer. A photodiode was used to measure the energy of each laser pulse. The particle size, pulse energy of the illuminating UV laser (263-nm or 351-nm), and the fluorescence information were all recorded for each particle simultaneously. The sizing of each detected aerosol particle was calibrated using National Institute of Standards and Technology (NIST) traceable polystyrene latex (PSL) microspheres aerosolized by a Royco aerosol generator (Model 256, Royco Instruments Inc.). Calibration PSL particles were distinguished from surfactant, dust and aggregate particles, by the associated UV-LIF data from the ICCD. The particle size distribution was also validated by an Aerodynamic Particle Sizer<sup>®</sup> Spectrometer (Model # 3321, TSI Inc.) during the calibration process.

Understanding the changes of fluorescence from BtAH and MS2 aerosols due to aging in a rotating drum was complicated by the fact that the size distribution of the aerosol typically changed during the exposure period. Changes in the aerosol size distribution were due to different sized particles being removed physically (by gravitational, inertial, and centrifugal forces) at different rates inside the rotating drum, with larger particles being removed faster than smaller particles. For a given material, the fluorescence intensity is dependent on the particle size (represented here by  $d$ , the diameter of a volume-equivalent sphere), particle shape, and the particle orientation relative to the excitation beam and collection optics. For all the particles and fluorescence emission wavelengths used in this paper, it was assumed that the fluorescence is proportional to absorption by a particle to within a few percent because re-absorption within the particle is small [10,14]. Then, the absorption by a particle and the fluorescence intensity are approximately proportional to particle volume ( $d^3$ ), i.e., to the number of fluorophores in a homogeneous particle, under the conditions where (i) the particle diameter is sufficiently small relative to the wavelength [33, 6.13 and 6.31]; (ii) or the real refractive index is near one and the absorptivity is small so that the particle is in the Rayleigh-Gans regime [33, 7.12]; or (iii) the particle (sphere or non-sphere) is not small, but the imaginary component of the refractive index is sufficiently small so that a plane wave propagating through the material could propagate many (e.g., 10) particle lengths  $L$  (where  $L$  is the maximum length of the particle) and not decrease in intensity ( $W/\text{m}^2$ ) more than a few percent, and the absorption is averaged over a range of sizes or wavelengths sufficient to smooth out the morphology-dependent resonances (MDRs), also known as whispering gallery mode resonances, in the absorption cross section [11]. In contrast, the absorption by a particle and fluorescence intensity is approximately proportional

to particle cross-sectional area (proportional to  $d^2$ ) in cases when the particle is highly absorbing so that a plane wave decreases to a small percentage (e.g., 4%) of its initial value when it propagates through a distance comparable to a particle diameter (or the smallest semi-axis of an ellipsoid). Particles between these two limiting cases are sometimes normalized by  $d^y$ , where  $y$  is some value typically between 1.9 and 3.2 [23,29]. For the data presented here, the fluorescence intensity for each particle was normalized for 263-nm excitation by dividing the fluorescence by  $d^{2.05}$ , and was normalized for 355-nm excitation by dividing the fluorescence by  $d^{2.8}$ , where the 2.05 and 2.8 were estimated from calculations of fluorescence versus diameter for dry homogeneous spherical particles which had concentrations and optical parameters similar to those obtained by Hill et al. [14]. If the concentrations and optical properties of the molecules in biological particles [14] are used to estimate fluorescence versus size, these approximate exponents appear to be useful, especially if the 263-nm excited particles contain a negligible amount of water.

## 2.2. Growth and preparation of biological aerosol materials

BtAH spores were obtained from MRI Global Inc. BtAH spores were spread-plated on New Sporulation Medium (NSM) agar, consisting of 0.3% Tryptone (Benton Dickinson and Co., Product # 211705), 0.3% yeast extract (Benton Dickinson and Co., Product # 212750), 0.2% agar (Benton Dickinson and Co., Product #214010), 2.3% Lab-Lemco agar (Oxoid Ltd., Product # CM0017), and 0.001%  $\text{MnCl}_2$  (Sigma-Aldrich Inc. Product # M8054) (w/v), and incubated for seven days at 37 °C [4]. The resulting bacteria lawn, which sporulated as nutrients were exhausted, was then scraped into 0.22  $\mu\text{m}$  sterile-filtered deionized (DI) water, and heat-shocked for ten minutes at 70 °C, to kill any remaining vegetative cells. The suspension was pelleted once by centrifugation at 4500 RPM for 25 minutes (Model # Allegra X-22R, Beckman-Coulter Inc.), to wash away any residual media and cellular debris, and then resuspended into sterile-filtered DI water. The suspension was further diluted in sterile-filtered DI water to achieve an aerosol particle diameter of approximately 2  $\mu\text{m}$ . The final concentration of BtAH spores in the aerosol suspension used for experiments was determined by culture to be 1.7E8 colony forming units per mL (CFU/mL).

Male-specific bacteriophage (MS2) (ATCC # 15597-B1) production and plaque assays utilized *Escherichia coli* str. C-3000 (ATCC # 15597) as the host organism. The recommended media, EM 271, was prepared by combining and autoclaving 1% tryptone (Benton Dickinson and Co., Product #211705), 0.1% yeast extract (Benton Dickinson and Co., 212750), and 0.8% NaCl (Sigma-Aldrich Inc., Product # S7653) (w/v). Agar (Benton Dickinson and Co., 214010) was added for solid medium at 1.5%, and the resulting autoclaved medium was supplemented with 0.1% glucose (Sigma-Aldrich Inc., Product # G5767), 0.0294%  $\text{CaCl}_2$  (Sigma-Aldrich, Product # C7902), and 0.001% thiamine (Sigma-Aldrich Inc., Product # T5941) w/v, all of which were 0.22  $\mu\text{m}$  sterile-filtered. *E. coli* C-3000 host cultures were propagated from glycerol stocks by overnight

incubation on EM 271 agar at 37 °C. Individual colonies were picked, placed into EM 271 broth, and incubated (37 °C, 200 RPM) until log-phase culture (spectrophotometric absorption between 0.2 and 0.5 at 520 nm) was achieved, as monitored by spectrophotometer (Model # Ultraspec 2100 Pro, Amersham Biosciences Corp.). Lyophilized MS2 stock was resuspended in EM 271, with 100  $\mu\text{L}$  used to inoculate the log-phase *E. coli*. Incubation of the suspension continued for eighteen hours, after which point the culture was centrifuged for 25 minutes at 4500 RPM (Beckman Coulter Allegra X-22R) to remove any residual *E. coli*. As a final cleanup, the MS2-containing supernatant was filtered using a 0.22  $\mu\text{m}$  filter to finish removing any large cellular debris. The resulting stock was further diluted in sterile-filtered DI water, in order to achieve a mean particle size of 2  $\mu\text{m}$  during aerosol experiments. The final concentration of MS2 used for aerosolization was determined to be 7.8E9 plaque forming units (PFU/mL).

The final suspensions of BtAH and MS2 were loaded daily into 30 mL syringes with magnetic stir bars for aerosolization.

## 2.3. Experimental details

Each measurement period lasted four hours, with additional time required for ozone conditioning. Prior to the test, the drum was pre-conditioned to an RH 5% below the desired value, to allow for additional moisture that was introduced into the drum by the wet-disseminated aerosol. Aerosols were generated and introduced into the chamber for ten minutes, to reach a particle concentration of 300 particles/ $\text{cm}^3$  or above. Once the aerosol had reached the desired concentration, initial measurements were made with the UV-APS and SPFS. An all-glass impinger (AGI-30, Ace Glass Inc.) operated for five minutes at 12.5 Lpm, collecting the bioaerosols into phosphate buffered saline. If the test required ozone conditioning, ozone was added to the drum for approximately 20 minutes after the initial measurements, until the ozone reached a concentration of  $\sim 150$  ppb. The four-hour measurement period thus began with UV-APS and SPFS measurements taken every hour. UV-APS samples were collected for three minutes every hour using a 30 second sampling cycle in the Aerosol Instrument Manager (AIM) software (AIM, TSI Inc.). The pump for the UV-APS was remotely powered off when not sampling. The SPFS was used to sample 200 particle spectra every hour. During the measurement period, ozone and RH generation systems were used to maintain the ozone and RH at their set points. For ozone, this control system was turned on for two minutes every ten minutes to maintain ozone levels during high ozone trials. Air lost during sampling for the AGI-30, UV-APS, SPFS, and ozone monitor was balanced with particle and vapor-free, filtered dry air that was sent into the drum using a mass flow controller (Model # MCR-250SLPM-D, Alicat Scientific Inc.). Between each measurement, while the aerosol was being aged, no air was introduced or withdrawn from the drum. Each time a sample was drawn from the drum chamber, the aerosol population was effectively diluted due to the influx of the

clean particle-free air to maintain pressure. In order to maintain a representative population for the four-hour experiments, AGI-30 samples were only taken at the start and end of each experiment due to the high flow rate (12.5 Lpm) required for sampling. At the end of the four-hour measurement period, final measurements were taken with the UV-APS and SPFS, and the final sample was collected by AGI-30. The drum was then purged at 55 Lpm for about 30 minutes, until the aerosol concentration was below 1% of its starting value.

BtAH spores and MS2 bacteriophage in *E. coli* lysate (described previously) were generated into the drum using suspensions that achieved a mean particle size of  $\sim 2 \mu\text{m}$ . Submicron particles are difficult for the light-scattering sizing of the SPFS to measure, and particles greater than  $3 \mu\text{m}$  are more rapidly lost in the drum physically over the four-hour period. In order to assess the changes in the biological activity of the aerosols, samples taken with the AGI-30 were enumerated via culture and quantitative polymerase chain reaction (q-PCR) immediately following aerosolization into the drum and at the end of each experiment. Due to the physical losses of particles during the experiments, culture alone could not be used to determine the changes in biological activity, because a perceived decrease in viability/infectivity could simply have been a drop in the number of sampled particles. Instead, the ratio of culturable organisms to genomic equivalents was used as an indicator of biological activity, assuming that the number of genomic equivalents per organism would not change during the course of the experiment.

Using three RH ( $\sim 80\%$ ,  $50\%$  and  $20\%$ ) and two-ozone concentrations ( $\sim 0$  and  $150 \text{ ppb}$ ), the fluorescence changes of the aerosol due to exposure to RH and ozone were measured independently and in combination. An exposure at  $150 \text{ ppb}$  for 4 hours in the drum represents the integrated EPA exposure limit for ozone during an 8-hour period and therefore represents a worst case scenario in an urban environment for which a biological aerosol could theoretically be exposed to aging for up to 8 hours. Each experimental condition was repeated three times.

#### 2.4. Determination of biological activity

The genomic content of samples containing BtAH was determined using q-PCR on an existing assay developed at the Johns Hopkins Applied Physics Laboratory (JHU/APL) for the *rpoB* gene on *Bacillus anthracis*. The probe uses a Quasar 570 fluorophore on the 5' end, with a BHQ-2 black hole quencher on the opposite 3' end. DNA isolations were accomplished via a five-minute bead beat using  $100 \mu\text{m}$  glass silica beads (MP Biomedicals LLC, Product #116911100), followed by a rapid gel cleanup using Bio-Spin 30 columns (Bio-Rad Laboratories Inc., Product # 732.). The assay was evaluated using a three-step PCR reaction on a Cepheid SmartCycler II system. Mastermix was developed using TaqMan Universal PCR Master Mix (Roche Diagnostics, Product # 4304437), with a ten-minute  $95^\circ\text{C}$  activation followed by 47 cycles consisting of  $95^\circ\text{C}$  melting,  $47^\circ\text{C}$  annealing, and  $60^\circ\text{C}$  extension temperatures. The primers and probe set were added to

the Mastermix at concentrations of  $300 \text{ nM}$  and  $250 \text{ nM}$ , respectively, and brought to a volume of  $20 \mu\text{L}$  with molecular biology grade water. The remaining  $5 \mu\text{L}$  of the reaction was reserved for the samples, which were analyzed in triplicate along a negative control, a standard curve dilution (based on the original aerosol stock), and no template controls for the DNA extraction process.

BtAH samples from the AGI-30s were additionally enumerated in triplicate by plating on Tryptic Soy Agar (TSA) plates using a Spiral Biotech Autoplate ( $50 \mu\text{L}$  exponential setting), and incubated overnight (sixteen hours) at  $37^\circ\text{C}$ . A Spiral Biotech Q-Count calculated the number of colonies and resulting viable concentrations (CFU/mL).

The infectious concentration of MS2 phage samples was determined by a plaque assay utilizing the same C-3000 strain of *E. coli* used in propagation. Single colonies of *E. coli* were inoculated into EM 271 and incubated ( $37^\circ\text{C}$ ,  $200 \text{ RPM}$ ) until reaching the log-phase. The *E. coli* was co-inoculated with  $0.5 \text{ mL}$  of serially diluted MS2 into EM 271 containing  $0.5\%$  agar, and kept melted in a  $46^\circ\text{C}$  water bath. The tube was then emptied onto EM 271 plates, incubated overnight at  $37^\circ\text{C}$ , and counted in the morning.

MS2 phage sample RNA concentrations were determined by quantitative real-time fluorescent reverse transcriptase polymerase chain reaction (RT-PCR). RNA from MS2 drum samples was isolated using a QIAamp viral RNA kit (Qiagen Inc., Product # 52904) and isolated in parallel with a standard curve based on serial dilutions from the original stock. Reverse transcriptase and PCR were accomplished in  $20 \mu\text{L}$  reactions, using an EXPRESS One-Step qRT-PCR Universal Mastermix (Life Technologies Inc., Product #11781). Primers and probes, targeting an assembly protein gene, were based on a set published by O'connell et al. [22]; FAM was the target dye, attached opposite a TAMRA quencher on the 5' end, with ROX serving as a passive reference at a concentration of  $500 \text{ nM}$ . Molecular biology grade water was added until the volume per well reached  $15 \mu\text{L}$ , with the remaining  $5 \mu\text{L}$  reserved for the sample. Complementary DNA synthesis occurred during a fifteen-minute hold at  $50^\circ\text{C}$ , followed by an activation at  $95^\circ\text{C}$  for 20 seconds, and 50 cycles of  $95^\circ\text{C}$  melting and  $60^\circ\text{C}$  annealing and extension temperatures. All the samples were run in triplicate on an ABI StepOne Plus, with no template controls for the PCR and RNA isolation processes, and a standard dilution curve.

The active fractions for both BtAH and MS2 were determined by dividing the number of viable/infectious organisms measured by the total genomic equivalents, with the initial aerosol stock used as a baseline, measured using qPCR.

### 3. Results

#### 3.1. Experimental conditions in the rotating drum system

Five experimental conditions were tested for each type of aerosol: RH Low, RH Medium, and RH High ( $20\%$ ,  $50\%$ , and  $80\%$ ), with ozone at either Low or High ( $0$  and  $150 \text{ ppb}$ ). The effects of temperature were not the focus of this study but were monitored to ensure that the

temperature was consistent. The temperature in the drum chamber during the experiments was stable at 20–21 °C with 3% variation across all experiments. During experiments where a low RH was desired, the average RH across all experiments was  $24 \pm 5\%$  with the RH slightly increasing during experiments. For experiments in which a medium RH was desired, the average RH across all experiments was  $52 \pm 3\%$ . The average high RH was  $81 \pm 3\%$ . The average low and high ozone concentrations once target levels were achieved inside the drum were  $6 \pm 3$  ppb and  $144 \pm 11$  ppb, respectively.

### 3.2. Size distributions of aerosols during experiments

The average size distribution of BtAH spore aerosols was multimodal for all experiments with a peak mode diameter of 1.8  $\mu\text{m}$ . During the 4-hour period, the peak mode shifted to a smaller diameter ( $\sim 1.6 \mu\text{m}$ ) as larger particles in the drum were lost faster than the smaller particles due to physical decay. Fig. 1(a) shows the size distributions of BtAH spores during the two extreme experimental conditions with low RH and low ozone concentration and high RH and high ozone. Both distributions are very similar at the start of experiments with the higher RH distribution being slightly less broad after 4 hours in the rotating drum, potentially due to particle uptake of water. Uptake of water would have resulted in larger particles, and subsequently larger physical losses in the drum.

The initial size distribution of MS2 phage aerosol varied more prominently as a function of RH than did the BtAH. The mode size at low RH was approximately 1.8  $\mu\text{m}$ , similar to that of the BtAH spores (Fig. 1(b)). At medium and high RH the mode sizes started at 2.2 and 2.5  $\mu\text{m}$ . These differences in the starting mode size indicate uptake of water by the MS2 aerosols in the rotating drum. EM271 media contains a large amount of NaCl that likely dominates the hygroscopic properties of the MS2 phage aerosol used for these experiments. The deliquescence relative humidity (DRH), defined as the RH in which an aerosol will begin to uptake water and the efflorescence relative humidity (ERH), the RH in which an aerosol will return to a crystalline state for NaCl are 73% and 45%, respectively [28]. It is probable that the aerosol introduced into the

drum was under slightly wet conditions after passing through the ACC and never fully reached the ERH in order to dry completely to a crystalline state. Given the average RH in the drum during the medium RH experiments was 52%, and the known ERH for NaCl is 45%, the MS2 phage aerosol was likely in transition phase, which explains the mode size of 2.2  $\mu\text{m}$  that falls between the low and high RH mode sizes. For experiments performed at high RH ( $> 80\%$ ) the slightly wetted aerosol entering the drum likely continued to uptake water to achieve a mode size observed at 2.5  $\mu\text{m}$  causing larger particles to be lost in the drum rapidly. As shown in Fig. 1(b), the mode size at high RH after 4 hours in the rotating drum is considerably shifted from about 2.5 to 1.1  $\mu\text{m}$  during a 4-hour experiment, while in relatively low RH conditions, the mode size remains at approximately 1.7  $\mu\text{m}$  throughout the 4-hour period.

### 3.3. Fluorescence of BtAH and MS2 phage measured with the SPFS

The SPFS was used to measure the fluorescence at excitation wavelengths 263 and 351 nm of BtAH and MS2 aerosols during the 4-hour experiments. The results are shown in Figs. 2–5. The data sets shown are the averages from three experiments and each plot represents 600 UV-LIF spectra from 200 individual aerosol particles during each of the three experiments. The fluorescence intensities were normalized by  $d^{2.05}$  or  $d^{2.8}$ , for fluorescence excited at 263 and 351 nm, respectively, in order to reduce the effects of the decrease in the average particle size, over the course of an experiment.

The integrated fluorescence over each emission band, plotted versus time for each experiment (shown in Figs. 6 and 7) illustrates more clearly the trends in amplitudes. The UV 263 is the integrated fluorescence band intensity from 280 to 400 nm when excited by a 263 nm laser. The Vis 263 is the fluorescence from 400 to 580 nm when excited by a 263 nm laser. The Vis 351 is the emission band from 380–700 nm when excited by a 351 nm laser.

Table 1 summarizes the measured decreases in integrated fluorescence from the initial time ( $t=0$  min) to the final time ( $t=4$  h) for the different emission bands, excitation wavelengths, and type of aerosol. The  $p$ -values

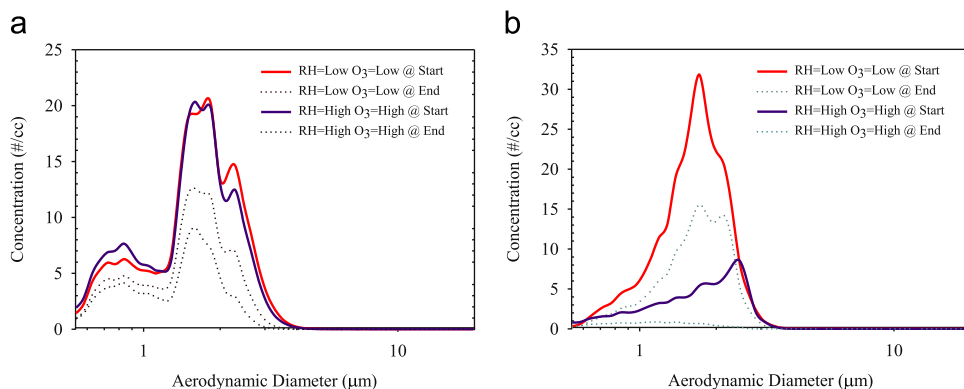
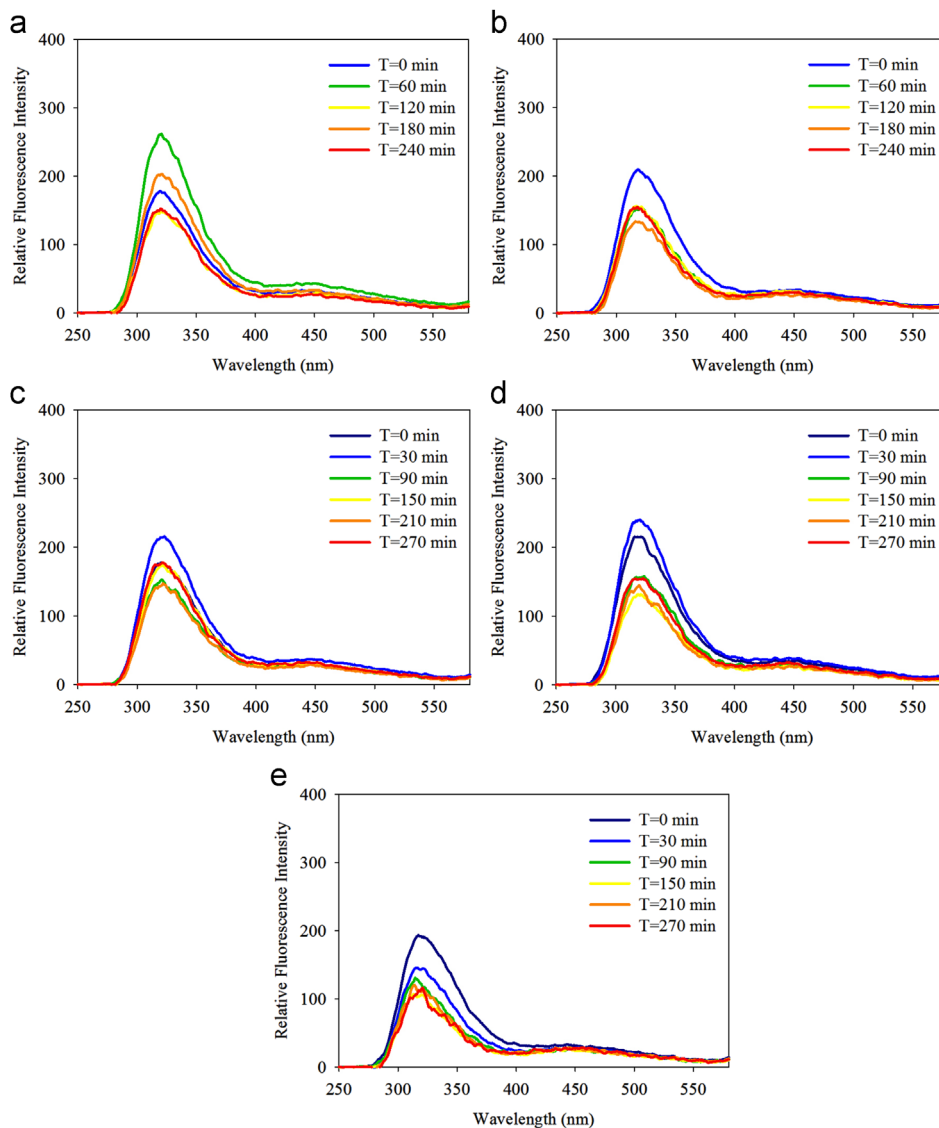


Fig. 1. (a) BtAH size distributions at the start and end of two types of experiments (b) MS2 size distributions at the start and end of two types of experiments.



**Fig. 2.** BtAH emission spectra as a function of time when excited at 263 nm for each exposure type. Each plot represents the average of 200 particle spectra at each time point for three experiments. (a) RH=Low,  $O_3$ =Low, (b) RH=High,  $O_3$ =0 Low, (c) RH=Low,  $O_3$ =High, (d) RH=Med,  $O_3$ =High and (e) RH=High,  $O_3$ =High.

calculated using the  $t$ -test with unequal variances is shown. It is the probability that the two sets of three measurements, initial and final, are sampled from the same distribution. The overlaps in the standard errors between the initial and final fluorescence intensities are calculated in order to help in estimating whether the decreases are significant. Decreases in fluorescence intensity are considered significant in the absence of an overlap of the error bars of the intensities measured at the initial and final time points.

For BtAH the averaged fluorescence spectra (280–580 nm) excited at 263 nm are shown in Fig. 2, with two emission peaks, centered near 330 and 450 nm. The time-dependence of the integrated intensities over these bands can be seen in the solid lines and the dotted lines in Fig. 6. At low RH with low ozone, no large differences in the

relative intensity between the two fluorescence bands are observable, and the decrease of the 330-nm band is not monotonic. At high RH the 330 nm band intensities decrease slightly faster than the 450 nm band intensities. In Fig. 3, the fluorescence spectra (365–700 nm) with a 351 nm excitation have very slight intensity decreases, as can also be seen from the dashed lines in Fig. 6 for VIS 351.

For MS2 phage with 263-nm excitation, the fluorescence peak around 330 nm decreases more than that from BtAH as shown in Fig. 4 and the solid line in Fig. 7. For MS2 phage, at low RH and low ozone, the relative fluorescence intensities between the UV and visible bands changed little over the 4-hour experimental duration, even though both bands were slightly decreased. At high RH and low ozone, a large decrease over time occurred in both fluorescence bands excited at 263 nm. At low RH and high ozone concentration,

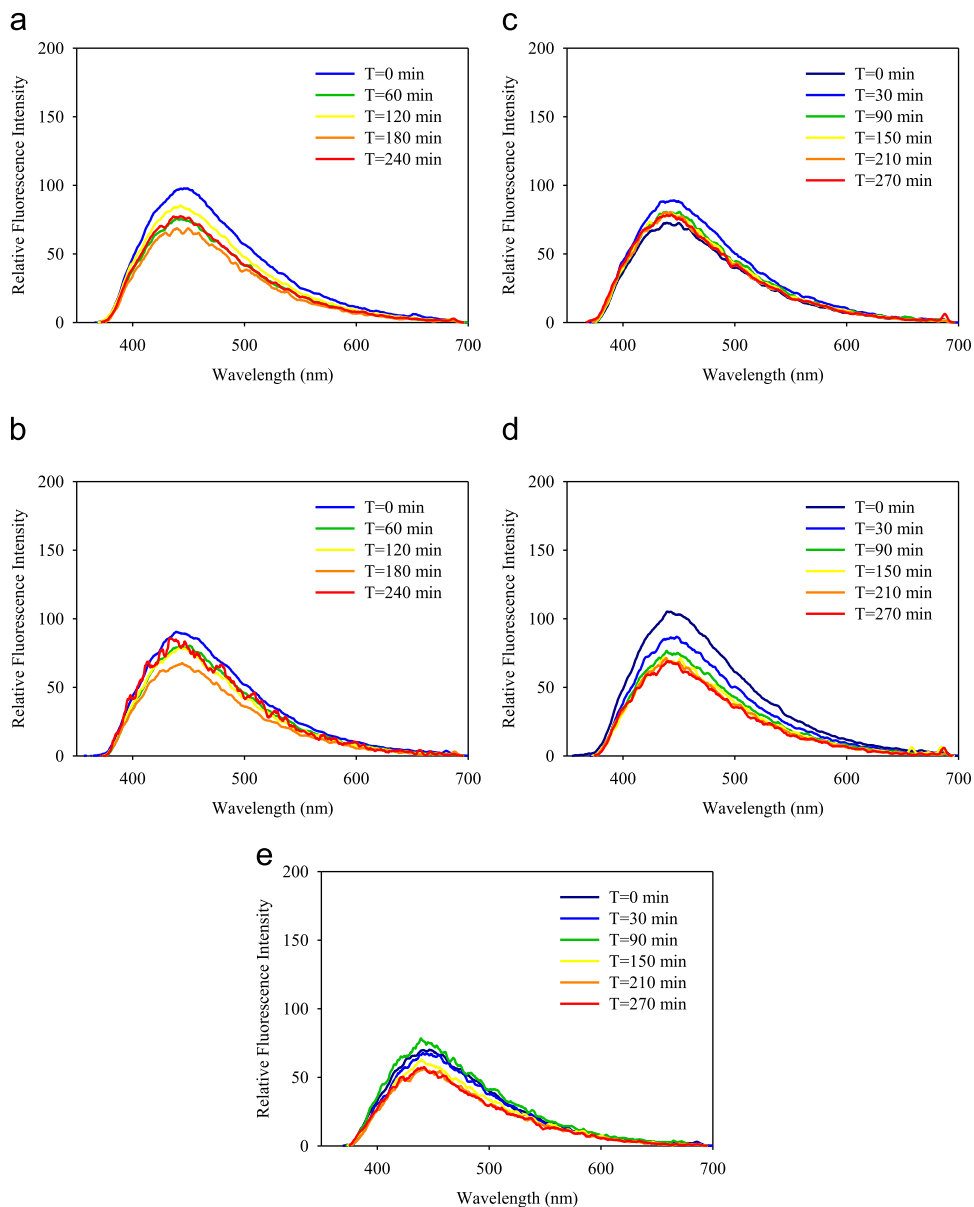


**Fig. 3.** BtAH emission spectra as a function of time when excited at 351 nm for each exposure type. Each plot represents the average of 200 particle spectra at each time point for three experiments. (a) RH=Low,  $O_3$ =Low, (b) RH=High,  $O_3$ =0 Low, (c) RH=Low,  $O_3$ =High, (d) RH=Med,  $O_3$ =High and (e) RH=High,  $O_3$ =High.

large decreases were also observed for both fluorescence bands, with  $p \leq 0.06$  in both cases. The rate of decrease in fluorescence increased as RH was increased, particularly for the tryptophan fluorescence band around 330 nm. This suggests that both RH and ozone contributed to the decrease in fluorescence intensity, and that ozone accelerates the decrease of the UV band. Fig. 5 shows the fluorescence emission profiles excited at 351 nm for the MS2 phage. The decrease in fluorescence is more notable in all cases where a high concentration of ozone is present. Meanwhile a large blue-shift was notable for the UV band at 263 nm excitation especially in the presence of high ozone concentrations.

For low ozone, as shown in Fig. 6a and b, BtAH spores exhibit no significant decrease in the average integrated

fluorescence intensity in any of the fluorescence emission bands measured, except for the UV263 at high RH with  $p=0.06$ . The average integrated visible fluorescence intensity (VIS263) of BtAH spores does not decrease significantly even at high ozone concentrations (Fig. 6c–e). The VIS 351 fluorescence band of BtAH spores at medium and high RH in the presence of high ozone decreases significantly by 38% and 20%, respectively. At medium and high RH levels in the presence of high ozone, the UV 263 fluorescence band for BtAH decreased significantly, with nearly 45% decrease at high RH (Fig. 6e) and close to 26% at medium RH (Fig. 6d and c). Decreases in fluorescence for BtAH aerosols appear to stabilize after about 150 minutes of exposure (Fig. 6).



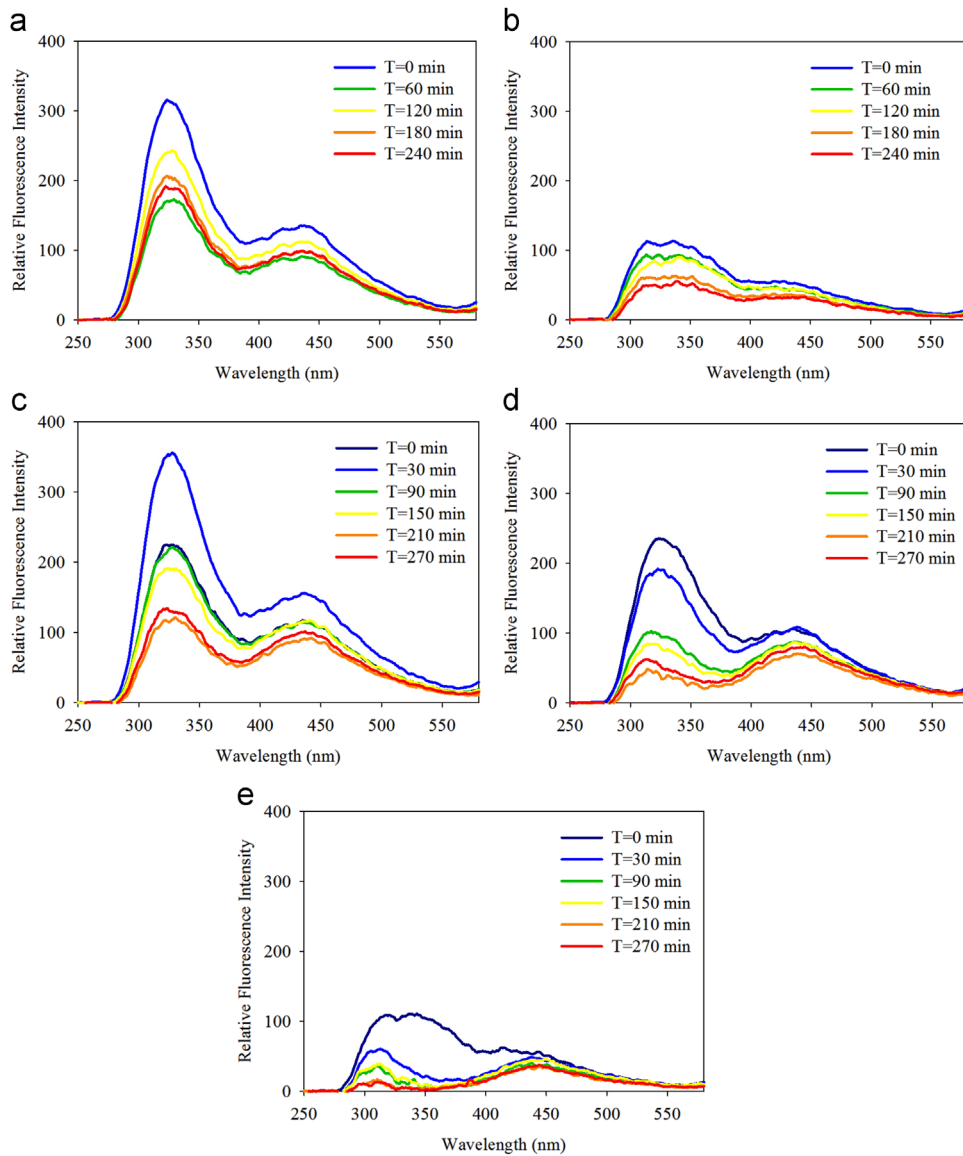


**Fig. 4.** MS2 emission spectra as a function of time when excited at 263 nm for each exposure type. Each plot represents the average of 200 particle spectra at each time point for three experiments. (a) RH=Low,  $O_3$ =Low, (b) RH=High,  $O_3$ =0 Low, (c) RH=Low,  $O_3$ =High, (d) RH=Med,  $O_3$ =High and (e) RH=High,  $O_3$ =High.

For MS2 at low RH and low ozone, shown in Fig. 7a, no decrease in the fluorescence intensity appears significant. At high RH and low ozone, neither of the VIS peaks for MS2 decreases significantly; however, the UV263 appears to be constant for the first 120 minutes then followed by a 38% decrease. The VIS263 nm fluorescence band for MS2 at high ozone does not decrease significantly for low and medium RH, but does decrease by 52% in the presence of high RH (Fig. 7e). At all RH in the presence of high ozone the UV 263 and VIS 351 all decrease significantly (Fig. 7c–e). As the RH increased from low to high in the presence of high ozone concentration, the intensity decrease of the UV 263 fluorescence band is monotonically increased (31% to 56% to 75%). The decreases of fluorescence from MS2 are more rapid than those from BtAH. The decrease was stabilized after the

first 100 minutes in the presence of high ozone and low RH, but changed fast when exposed to high ozone and high RH and stabilized after about 50 minutes.

#### 3.4. Fluorescence of Bt Al Hakam and MS2 phage measured with UV-APS

Shown in Fig. 8a is the average fluorescence intensity of BtAH spores for different experimental conditions over time for the 1.8  $\mu\text{m}$  size bin measured by UV-APS. Unlike the SPFS measurements, the fluorescence increased with time with no apparent change in the rate of increase as a function of ozone or RH. In all cases, the fluorescence appears to initially decrease between 0 and 30 minutes (for experiments where ozone was introduced into the chamber) and 0 and 60

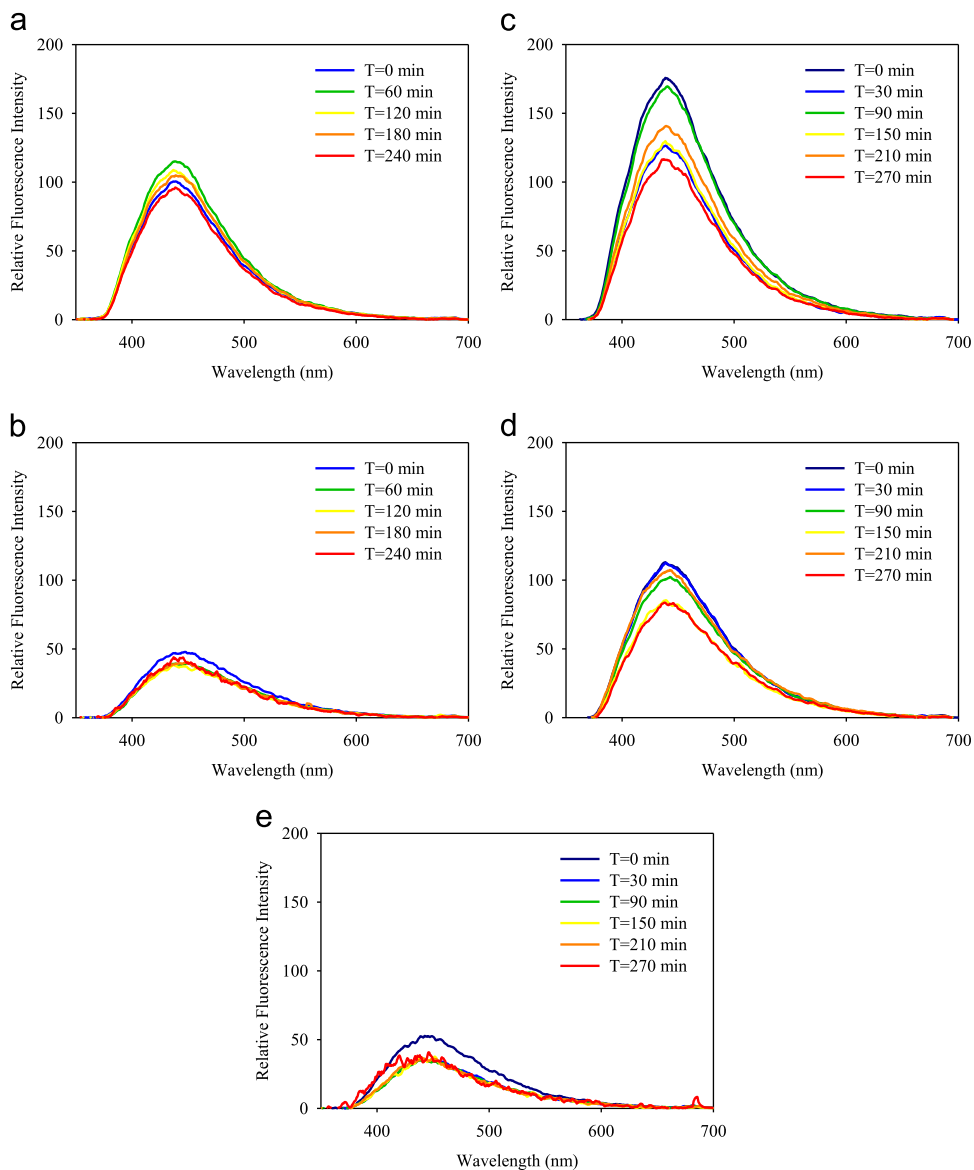


**Fig. 5.** MS2 emission spectra as a function of time when excited at 351 nm for each exposure type. Each plot represents the average of 200 particle spectra at each time point for three experiments. (a) RH=Low,  $O_3$ =Low, (b) RH=High,  $O_3$ =0 Low, (c) RH=Low,  $O_3$ =High, (d) RH=Med,  $O_3$ =High and (e) RH=High,  $O_3$ =High.

minutes where no ozone was present. This difference may be due to the degree of drying of the aerosol in the drum when the first measurement was taken at time “zero” versus the second time point after which equilibrium was reached. In general, the fluorescence is stronger at low RH than at high RH at all time points, a difference that is consistent with more water in the particles at higher RH. The rate of increase of fluorescence intensity shows little correlation between ozone concentration and RH.

For MS2 phage aerosol, some fluorescence trends can be seen with the experimental conditions. Shown in Fig. 8b are the average fluorescence intensities in the 2.0  $\mu\text{m}$  size bin for MS2 aerosols. First, RH was anticorrelated with the initial fluorescence. This is consistent with the presence of

additional water in these aerosols affecting the fluorescence intensity. One possible explanation for this difference in the starting fluorescence of both BtAH and MS2 aerosols; it could be that particles entering the drum under wet conditions grow almost instantaneously, before being measured by the UV-APS. This theory is consistent with the particles in the 1.8–2.0  $\mu\text{m}$  bins being much smaller when injected into the drum and then growing to that size at the higher RH. Particles entering the drum under dry conditions (at low RH) were 1.8–2.0  $\mu\text{m}$  to start and therefore grew little if at all. Therefore, a particle with a certain size (2.0  $\mu\text{m}$ ) at high RH contains less fluorescent material and more water than a particle of the same size at low RH, which started at 2.0  $\mu\text{m}$  and grew only little by the adsorption of water.

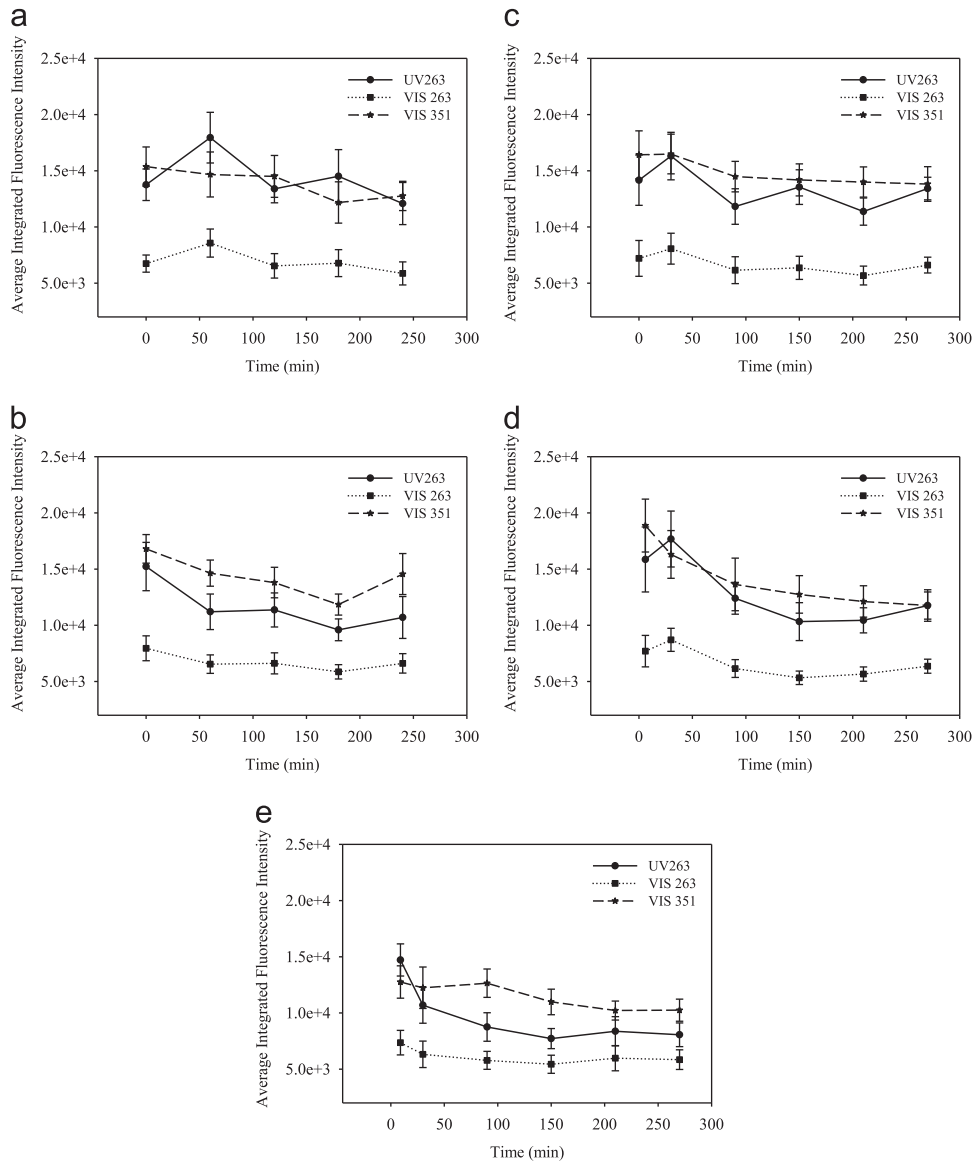


**Fig. 6.** Integrated fluorescence of BtAH aerosols in each of the three emission bands when excited at either 263 or 351 nm. UV 263 band=280–400 nm at excitation 263 nm, Vis 263=400–580 nm at excitation 263 nm, Vis 351=380–700 nm at excitation 351 nm. (a) RH=Low, O<sub>3</sub>=Low, (b) RH=High, O<sub>3</sub>=Low, (c) RH=Low, O<sub>3</sub>=High, (d) RH=Med, O<sub>3</sub>=High and (e) RH=High, O<sub>3</sub>=High.

### 3.5. Changes in biological activity of BtAH and MS2 phage

The change in biological activity (viability for BtAH and infectivity for MS2) during experiments was measured to determine what effects exposure to ozone and RH may have on the functionality of the aerosols. The approach taken for these experiments was to measure the biological activity against the total genomic equivalents present in the aerosol samples. In theory, if there is no change in biological activity (biological decay), then the ratio of active units to genomic equivalents should stay the same regardless of physical losses. The culture of samples taken with AGI-30 at the start and the end of each experiment were compared with q-PCR to

determine if any biological decay could be observed. Fig. 9 shows the arithmetic mean log change in biological activity at different experimental conditions. In the case of MS2 phage, a 2–3 log loss in infectivity (of *E. coli* cells) was observed for medium or high RH in the presence of high ozone concentration. The change in BtAH is less straightforward. These experiments showed an apparent increase in viable fraction under high ozone conditions. It is not feasible that the BtAH was replicating during the 4-hour experiments in the aerosol state, and therefore, the number of genomic equivalents must be decreasing. The decrease in infectivity of MS2 phage is consistent with the decrease in fluorescence intensity measured by SPFS.

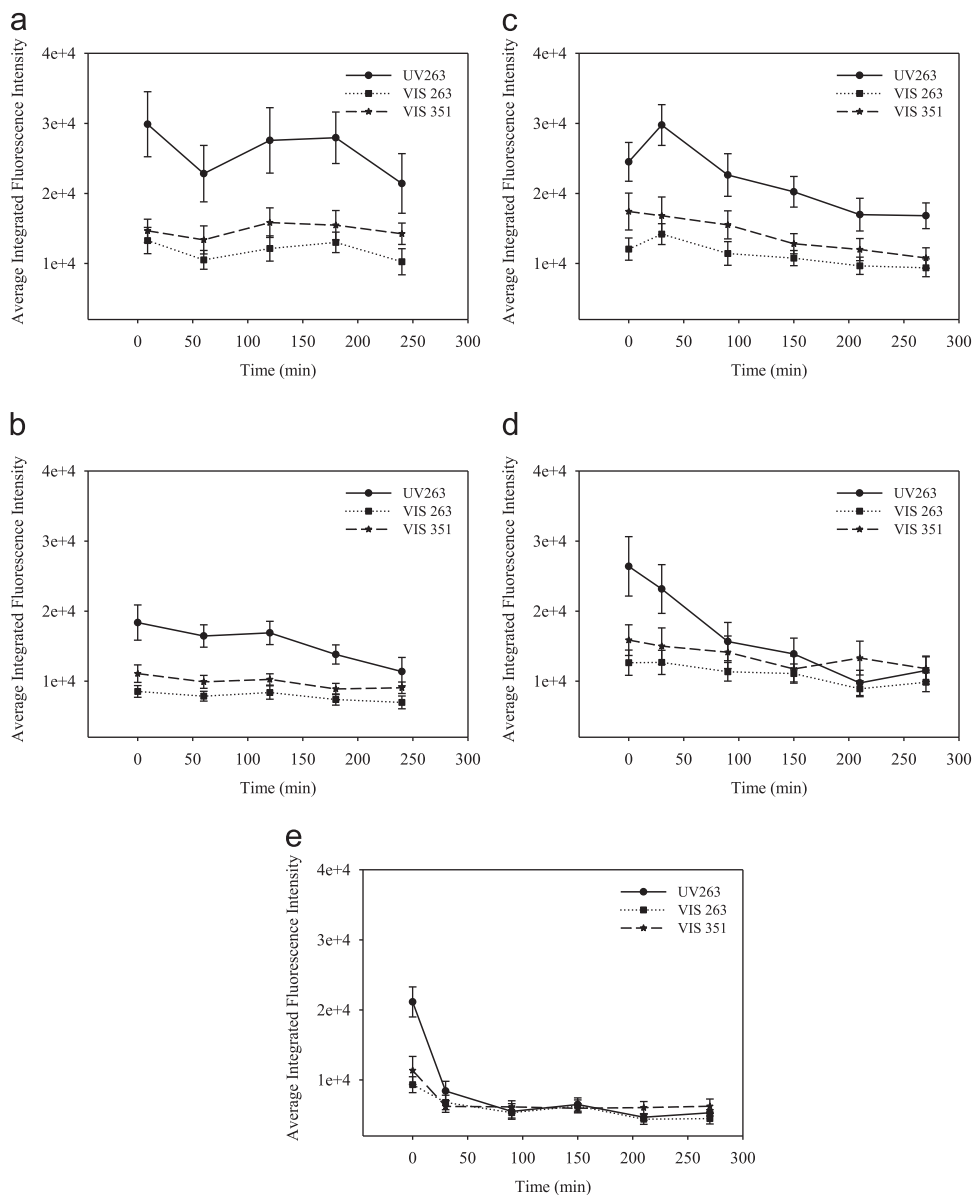


**Fig. 7.** Integrated fluorescence of MS2 aerosols in each of the three emission bands when excited at either 263 or 351 nm. UV 263 band=280–400 nm at excitation 263 nm, Vis 263=400–580 nm at excitation 263 nm, Vis 351=380–700 nm at excitation 351 nm. (a) RH=Low,  $O_3$ =Low, (b) RH=High,  $O_3$ =0 Low, (c) RH=Low,  $O_3$ =High, (d) RH=Med,  $O_3$ =High and (e) RH=High,  $O_3$ =High.

#### 4. Discussion

Fluorescence between 320 and 350 nm in bacteria and proteins is attributed to the presence of tryptophan when excited by light between 250 and 290 nm [14,23,26]. When oxidized by ozone in liquid solution and in animal tissues, tryptophan fluorescence at  $\sim 330$  nm decreases as oxidation and reaction with water result in the formation of NFK and NK [24] both of which fluoresce between 400 and 420 nm [23,26]. Previous studies performed by [26] with MS2 and *Yersinia rhodei* aerosols show similar results to these experiments in which treatment with ozone leads to a

decrease in the 330 nm band relative to the 400–580 nm band, especially in the case of MS2 phage aerosols at high RH and high ozone concentration. However, in these experiments no increase in fluorescence was observed that would indicate the production of kynuerine products. Given the complexity of the molecular composition of bioaerosols and the possible oxidation products, it is possible that while some fluorophores are being oxidized and their fluorescence intensity is decreased in the visible band by 351 nm excitation, fluorescence intensity may be increased from the generation of new fluorophores by products of oxidation, and result in a net effect that has little change in fluorescence intensity by 351 nm excitation.

**Table 1**

Percent decrease in fluorescence in each emission band for BtAH and MS2 as function of ozone concentration and relative humidity.

Em Exc	RH	Bt Al Hakam						MS2 bacteriophage					
		Low ozone			High ozone			Low ozone			High ozone		
		Decr.%	$(F_F - F_i) / (SD_F + SD_i)$	<i>p</i>	Decr.%	$(F_F - F_i) / (SD_F + SD_i)$	<i>p</i>	Decr.%	$(F_F - F_i) / (SD_F + SD_i)$	<i>P</i>	Decr.%	$(F_F - F_i) / (SD_F + SD_i)$	<i>p</i>
UV 263	Low	12	0.51	0.22	5	0.23	0.71	28	0.95	0.09	31	1.67	0.03
	Med	—	—	—	26	1.001	0.16	—	—	—	56	2.40	0.012
	Hi	30	1.13	0.06	45	2.68	0.005	38	1.54	0.03	75	6.13	0.001
	Avg.	21	0.82	—	25	1.30	—	33	1.25	—	54	3.40	—
VIS 263	Low	13	0.49	0.23	8	0.26	0.67	23	0.81	0.12	22	0.94	0.11
	Med	—	—	—	17	0.66	0.31	—	—	—	22	0.89	0.13
	Hi	17	0.68	0.21	21	0.77	0.17	18	0.90	0.08	52	2.54	0.006
	Avg.	15	0.59	—	15	0.56	—	21	0.86	—	32	1.46	—
VIS 351	Low	17	0.86	0.14	16	0.71	0.21	3	0.13	0.77	38	1.62	0.04
	Med	—	—	—	38	1.89	0.02	—	—	—	26	1.02	0.08
	Hi	13	0.72	0.097	20	1.04	0.10	18	0.97	0.12	45	1.68	0.036
	Avg.	15	0.79	—	25	1.21	—	11	0.55	—	36	1.44	—

Numbers in italics have no overlap of the error bars at the initial and final times, i.e., the difference between the initial and final average is greater than the sum of the standard deviations, or the case of *p* values, *p* is less than 0.1.

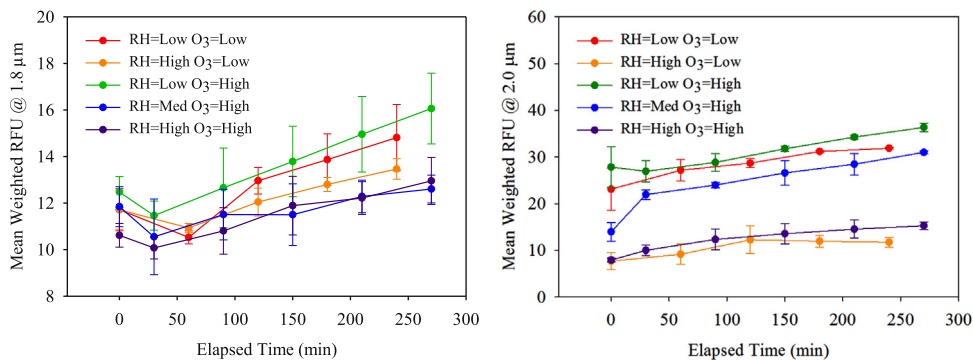


**Fig. 8.** (Left) Change in mean weighted fluorescence for BtAH spores at 1.8  $\mu\text{m}$ . (Right) Change in mean weighted fluorescence for MS2 phage at 2.0  $\mu\text{m}$ , both with UV-APS at 355 nm excitation.

It was expected that similar fluorescence spectral profiles and intensity would be produced by the excitation of similar molecules provided that the two fluorescence spectrometer systems, the SPFS and UV-APS, have similar excitation wavelengths (only 4 nm difference). In particular, the SPFS VIS351 emission covers the fluorescence from 365 to 700 nm, which decreases for BtAH and MS2 phage, with the largest decrease at high RH and high ozone concentration. The fluorescence emission (430–580 nm) observed by UV-APS increased over time for both BtAH and MS2 (with the exception of BtAH in the first 60 minutes) for all conditions tested. We could not find significant evidence for the hypothesis that the difference in the detection wavelength range for SPFS (365–700 nm) and UV-APS (430–580 nm) could explain this observed difference in the trends in fluorescence over time.

The data in Figs. 2–7 and Table 1 indicate that greater fractions of the fluorophores are modified by ozone in MS2 than in BtAH spores. The different rate of decrease observed for BtAH spores versus the MS2 phage indicates different kinetics are involved within the oxidation process for the

two types of aerosols during exposure to ozone. *Bacillus* spores contain a protective exosporium that likely shields the bacterium from oxidative stresses and slows the uptake of water. *Bacillus* spores are hydrophobic, and so in the absence of media or other material that might attract water molecules to the surface, the observed chemical changes due to ozone are expected to take longer with less intense reaction. Conversely, for MS2 phage, several factors may have contributed to the more rapid reactivity. MS2 phage aerosol preparation was filtered with a 2- $\mu\text{m}$  filter, but would have contained residual lysate from the *E. coli* cells (the parts of the lysate small enough to pass through the filter) and the now-spent EM271 media, containing NaCl, in which it was grown. Therefore a large fraction of the biological material in the MS2 aerosol is bacterial material that is not protected by a cell membrane. The NaCl in the media likely resulted in large uptake of water and therefore a higher probability of hydrolysis and oxidative damage during the aging process. Second, the MS2 phage does not contain the same protective factors as a spore (spore coat, calcium dipicolinate, or special soluble proteins) to protect

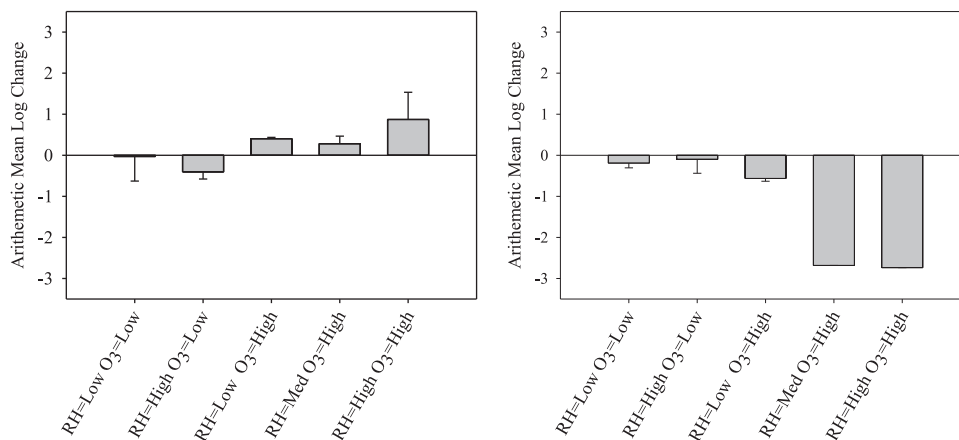


Fig. 9. (Left) Change in measured viability for BtAH spores during experiments. (Right) Change in measured infectivity for MS2 phage.

it from oxidative or other chemical reactants allowing more opportunity for the fluorophores in the MS2 aerosols to react and at a faster rate.

The loss in infectivity of MS2 appears to follow the same trend as the loss in fluorescence when excited at 263 nm for MS2 phage. This result is consistent with the protein degradation, which causes the decrease in the fluorescence, being the cause, or one of the causes, of the decrease in infectivity, but it could also be consistent with ozone damage to DNA being more responsible for the decrease in infectivity. The apparent increase in BtAH viability during high ozone experiments was initially perplexing. Untreated spore preparations have been shown to contain significant amounts of extracellular DNA, which in the absence of cell lysis treatment prior to assay may result in amplification of DNA during PCR [18]. DNA is known to react with ozone [3,31]. It is possible that extracellular DNA was oxidized and destroyed during experiments and resulted in a lower genomic material available for q-PCR. This would result in the ratio between culturable spores and genomic equivalents to decrease, regardless of changes in viability. These results indicate that the use of q-PCR (measurement of total genomic equivalents in a sample) as a method of normalizing for physical loss, in these types of experiments, may not be the most appropriate method for determining biological decay of *Bacillus* spores.

The results presented here also suggest that research studies or sensor technologies that use PCR-based detection for enumeration may be skewed if ozone or other atmospheric constituents destroy extracellular DNA more rapidly than intracellular materials (such as those in the core of a BtAH spore). The viability (infectivity of *E. coli* cells) of MS2 phage decreased by 100-fold while the average fluorescence intensity measured by the SPFS decreased by no more than 75% and the fluorescence intensity measured by the UV-APS increased by 30–45%. These results suggest additional studies are needed to understand the effects of atmospheric air on the ability of other detection modalities, such as antibodies to detect specific antigens of biological particles to correlate with biological activity and fluorescence.

The changes in fluorescence observed in the presence of different RH and ozone indicate that biological aerosols can be significantly altered while remaining aloft in the ambient environment. Laboratory studies, related to the characterization of biological aerosols and to the development of new sensor technologies, typically utilize aerosols measured shortly after aerosolization. The results of the studies shown in the present paper indicate that the fluorescence amplitudes and spectral profiles may be considerably different for freshly generated aerosols as compared with those that have been in the environment. The different conditions tested were intended to be representative of EPA standards for ozone exposure during an 8-hour period. The results suggest that at these levels, which often exist in urban areas, the changes observed may occur between 30 minutes and 3 hours following the emission of a biological particle into the atmosphere. Fluorescence based technologies used for measurement or detection of biological particles may therefore be misrepresenting actual atmospheric bioaerosol concentrations. For example, instruments that rely on tryptophan fluorescence (excitation in the range of 260–290 nm and measured fluorescence between 320 and 350 nm) may not accurately measure many bioaerosols that have been exposed to ozone and humidity. Additionally, the loss of extracellular genomic material on *Bacillus* spores during exposure may be an indication of a loss in sensitivity for sensors that utilize PCR based assays for detection and also be indicative of the potential for other extracellular components used for detection (such as antigen/antibodies) to be diminished.

## 5. Summary

The measurement and detection of biological aerosols in the atmosphere continues to be a topic of great interest in the scientific community. Most sensors for detecting biological aerosols rely on the presence of specific molecules in the biological particles, e.g., as antigens on the surface, DNA sequences, or molecules more common to all living cells such as tryptophan, flavins, or NADH, which can be detected in the intrinsic fluorescence of biological materials. In developing and testing bioaerosol detection methods, researchers

should account for the potential changes in the physical and chemical properties of bioaerosols caused by various atmospheric conditions. This paper describes experiments performed to measure the changes in light-induced fluorescence spectra and viability of two types of biological aerosols, BtAH and MS2. The aerosols were exposed for 4 hours in a rotating drum chamber to high and low RH at two ozone concentrations. Changes in fluorescence and viability were measured using an SPFS, UV-APS, cell culture, and q-PCR. For both BtAH and MS2 bioaerosols (i) the decrease in fluorescence intensity was larger when excited at 263 nm than when excited at 351 or 355 nm; (ii) the fluorescence of BtAH decreased more slowly, and with a much smaller net decrease, than did the fluorescence of MS2; (iii) the decrease in fluorescence of MS2 or BtAH was typically largest in the UV263 emission band, smaller in the VIS 351 band, and smallest in the VIS 263 band. Most of the decrease in fluorescence occurred in the first 100–150 minutes with BtAH spores, and in the first 50–100 minutes with MS2. The UV-APS fluorescence increased during experiments, but the SPFS fluorescence in the VIS 351 band decreased. This may be due to differences in the way the two instruments measure particle size, the differences in excitation wavelength or the range over which the fluorescence is integrated, however, not enough information was available to draw any specific conclusion. An approximately 2-log loss in viability was observed for the MS2 phage when it was exposed to ozone in the presence of high RH. The BtAH viability was skewed by the destruction of extracellular DNA and was therefore not quantifiable during experiments. This observation suggests that utilization of PCR based detection for *Bacillus* spores, may be limited if the spores have been exposed to atmospheric oxidizing agents. The results of these experiments indicate that the fluorescence spectra and viability (of BtAH) and infectivity (of MS2) of biological aerosols exposed for up to 4 hours to ozone at medium and high RH, which are not uncommon in the atmosphere, are different from those of freshly generated bioaerosols.

## Acknowledgements

The authors would like to thank Dr. Sari Paikoff at the Defense Threat Reduction Agency for providing the funding for this research.

## References

- [1] Ariya Parisa A, Amyot Marc. New directions: the role of bioaerosols in atmospheric chemistry and physics. *Atmos Environ* 2004;38:1231–2 (Web).
- [2] Benbough JE, Hood AM. Virucidal activity of open air. *J Hyg* 1971;69(04):619 (Print).
- [3] Cataldo Franco. DNA degradation with ozone. *Int J Biol Macromol* 2006;38(3–5):248–54 (Print).
- [4] Cliff JB, Jarman KH, Valentine NB, Golledge SL, Gaspar DJ, Wunschel DS, et al. Differentiation of spores of *Bacillus subtilis* grown in different media by elemental characterization using time-of-flight secondary ion mass spectrometry. *Appl Environ Microbiol* 2005;71(11):6524–30 (Print).
- [5] Cox CS, Hood AM, Baxter Jean. Method for comparing concentrations of the open-air factor. *Appl Microbiol* 1973;26(4):640–2 (Print).
- [6] Deguillaume L, Leriche M, Amato P, Ariya PA, Delort AM, Poschl U, et al. Microbiology and atmospheric processes: chemical interaction of primary biological aerosols. *Biogeosciences* 2008;5:1073–84 (Print).
- [8] Eversole J, Cary WK, Scotto CS, Pierson R, Spence M, Campillo AJ. Continuous bioaerosols monitoring using UV excitation fluorescence: outdoor test results. *Field Anal Chem Technol* 2001;15(4):205–12 (Web).
- [10] Hill SC, Pinnick RG, Niles S, Fell FF, Pan YL, Bottiger J, et al. Fluorescence from airborne microparticles: dependence on size, concentration of fluorophores, and illumination intensity. *Appl Opt* 2001;40(18):3005–13 (Web).
- [11] Hill Steven C. Method for integrating the absorption cross sections of spheres over wavelength or diameter. *Appl Opt* 2003;42(21):4381 (Web).
- [12] Hill SC, Pinnick RG, Pan YL, Holler S, Change RC, Bottiger J, et al. Real-time measurement of fluorescent spectra from single-airborne biological particles. *Field Anal Chem Technol* 1999;4–5(SI.3):221–39 (Web).
- [13] Hill Steven C, Pinnick Ronald G, Nachman Paul, Chen Gang, Chang Richard K, Mayo Michael W, et al. Aerosol-fluorescence spectrum analyzer: real-time measurement of emission spectra of airborne biological particles. *Appl Opt* 1995;34(30):7149 (Print).
- [14] Hill Steven C, Pan Yong-Le, Williamson Chatt, Santarpia Joshua L, Hanna H Hill. Fluorescence of bioaerosols: mathematic model including primary fluorescing and absorbing molecules in bacteria. *Opt Express* 2013;21(19):22285–313 (Web).
- [15] Hinds William C. *Aerosol technology: properties, behavior, and measurement of airborne particles*. New York: Wiley; 1999 (Print).
- [16] Ignatenko AV, Tatarinov BA, Khovratovich NN, Khrapovitskii VP, Cherenkevich SN. Spectral fluorescent investigation of the action of ozone on aromatic amino acids. *Zhurnal Prikl Spektrosk* 1982;37(1):64–8 (Web).
- [17] Ignatenko AV. Use of the method of tryptophan fluorescence to characterize disruptions of the structure of ozonized proteins. *J Appl Spectrosc* 1988;49.1:691–5 (Web).
- [18] Johns M, Harrington L, Titball RW, Leslie, DL. Improved methods for the detection of *Bacillus anthracis* spores by the polymerase chain reaction. *Lett Appl Microbiol* 1994;18(4):236–8 (Print).
- [19] May KR, Druett HA, Packman LP. Toxicity of open air to a variety of microorganisms. *Nature* 1969;221:1146–7 (Web).
- [20] Mik GDe, De Groot Ida. Mechanisms of inactivation of bacteriophage  $\phi$ X174 and its DNA in aerosols by ozone and ozonized cyclohexene. *J. Hyg* 1977;78.02:199 (Print).
- [21] Mudd JB, Leavitt R, Ongun Alpaslan, McManus TT. Reaction of ozone with amino acids and proteins. *Atmos Environ* 1969;3(6):669–81 (Web).
- [22] O'connell KP, Bucher JR, Anderson PE, Cao CJ, Khan AS, Gostomski MV, et al. Real-time fluorogenic reverse transcription-PCR assays for detection of bacteriophage MS2. *Appl Environ Microbiol* 2006;72(1):478–83 (Print).
- [23] Pan Yong-Le, Santarpia Joshua L, Ratnesar-Shumate Shanna, Corson Elizabeth, Eshbaugh Jonathan, Hill Steven C, et al. Effects of ozone and relative humidity on fluorescence spectra of octapeptide bioaerosol particles. *J Quant Spectrosc Radiat Transf* 2014;133:538–50 (Web).
- [24] Pryor WA, Uppu RM. A kinetic model for the competitive reactions of ozone with amino acid residues in protein in reverse micelles. *J Biol Chem* 1993;268(5):3120–6 (Web).
- [25] Ratnesar-Shumate Shanna A, Wagner Michael L, Kerechanin Charles, House Gerard, Brinkley Kelly, Bare Christopher, et al. Improved method for the evaluation of real-time biological aerosol detection technologies. *Aerosol Sci Technol* 2011;45(5):635–44 (Print).
- [26] Santarpia Joshua L, Pan Yong-Le, Hill Steven C, Baker Neal, Cottrell, McKee Laura, et al. Changes in fluorescence spectra of bioaerosols exposed to ozone in a laboratory reaction chamber to simulate atmospheric aging. *Opt Express* 2012;20(28):29867–81 (Print).
- [27] Schroder KL, Hargin PJ, Schmitt DJ, Rader DJ, Shokair IR. Development of an unattended ground sensor for ultraviolet laser-induced fluorescence detection of biological agent aerosols. *Proc SPIE* 1999;3855:82–91 (Web).
- [28] Seinfeld John H, Pandis Spyros N. *Atmospheric chemistry and physics: from air pollution to climate change*. New York: Wiley; 1998 (Print).
- [29] Sivaprakasam Vasanthi, Huston Alan L, Scotto Cathy, Eversole Jay D. Multiple UV wavelength excitation and fluorescence of bioaerosols. *Opt Express* 2004;12(19):4457 (Print).
- [30] Sun Jiming, Ariya Parisa A. Atmospheric organic and bio-aerosols as cloud condensation nuclei (CCN): a review. *Atmos Environ* 2006;40:795–820 (Print).

- [31] Theruvathu Jacob A, Flyunt Roman, Aravindakumar Charuvila T, Von Sonntag Clemens. Improved methods for the detection of *Bacillus anthracis*. *J R Soc Chem Perkin Transm* 2001;2:269–74 (Web).
- [32] Tilley RI, Ho J, Eamus D. Background bioaerosols and aerosols at two sites in northern Australia: preliminary measurements. Report No. DTSO-TR-1203. N.p. National Technical Information Service-Defense Technical Information Center, 2001. Print.
- [33] Van De Hulst HC. Light scattering by small particles. Reprint ed. N.p. Dover Publications; 1981 (Print).
- [35] Wilson GA, Defreeze RK. Autofluorescence detection using UV diode laser simultaneous excitation of multiple wavelengths. *Proc SPIE* 2003;5071:253–63 (Web).